

Refraction corrected transmission imaging based on Bézier curves: first results with KIT 3D USCT

F. Zuch¹, T. Hopp¹, M. Zapf¹, and N.V. Ruiter¹

¹ *Karlsruhe Institute of Technology, Karlsruhe, Germany, E-mail: franziska.zuch@kit.edu*

Abstract

The computational complexity of wave-based image ultrasound transmission reconstructions is very high especially in 3D. Hence, ray-based approximations are often used. Bent ray approaches like the fast marching method are time-consuming in comparison to the straight ray approximation. The Bézier curve technique for refraction approximation, introduced by Perez-Liva et al., could be a compromise between computational effort and image quality. In this work, the method was extended to 3D and an evaluation on two 3D datasets was carried out. The first dataset was simulated with the k-wave toolbox, with hemispherically arranged emitters and receivers and a sound speed inhomogeneity. With a mean squared error of 9.98 m/s the method produces similar results as the fast marching method (11.85 m/s). The object size is represented better in comparison to the straight ray method. Applied to real data of the KIT 3D USCT both methods performed similarly. The object size was better preserved using bent ray methods. The Bézier bent ray method shows first promising results in 3D as it leads to similar results than the fast marching method.

Keywords: USCT, transmission reconstruction, Bézier curve

1 Introduction

Ultrasound computer tomography is a new imaging modality for breast cancer detection [1]. Both transmission and reflection information can be obtained. Transmission images provide quantitative information about tissue properties like sound speed and attenuation [2, 3]. The focus of this paper is on the sound speed reconstruction as part of the transmission tomography.

For the image reconstruction, the wave propagation through tissue needs to be described (forward model) and an inverse problem needs to be solved for the image given the measured pressure fields and the forward model. The computational complexity of wave-based

image reconstructions is very high, especially in 3D at high frequencies [4]. For this reason, approximations are required. Here, ray-based approaches are commonly used to describe the path of propagation between emitter and receiver. The straight ray approximation neglects physical effects like refraction. Bent ray approaches like the widely used fast marching method [5, 6] may include this effect yet are still computationally demanding [7], especially in 3D.

Pérez Liva et al. [3, 7] introduced a ray-based method where a single refraction is approximated with a quadratic Bézier curve. The idea is that including the refraction of the water-tissue interface leads already to an improvement. A brute force search for the fastest curve out of a set of Bézier curves with different curvature connecting emitter and receiver is applied. The presented method was developed for the application in 2D. In this paper it is expanded to 3D, for the use on KIT 3D USCT, and an evaluation for 3D datasets is carried out.

2 Methods

2.1 Bent ray calculation with Bézier polynomial

The basic idea of Pérez Liva et al. [3] is to link two points, which in USCT are emitter and receiver, with a curve described by an Bézier polynomial [8]. For such a curve the sound speed map is used to derive the time of flight (TOF) of an ultrasound pulse travelling along this curve. Using a brute force search the curve with lowest TOF is determined.

For implementation in 3D, we consider a quadratic Bézier curve, discretized by t , which is described by the following equation:

$$C(t) = (1-t)^2P_0 + 2t(1-t)P_1 + t^2P_2, t \in [0, 1]. \quad (1)$$

P_0 , P_2 correspond to the start- and endpoint of the curve. In 3D USCT these positions are given by the emitter and receiver coordinates. P_1 is a free point. It controls the curvature of the Bézier curve. By moving this control point, different curves between emitter and receiver can be generated. The free points P_1 are distributed along and vertical to the direct line connecting emitter and receiver in order to derive a set of possible curves connecting P_0 and P_2 . The distribution was calculated via linear equation from the emitter-receiver-centre with the given direction vectors (see Fig. 1 (a)):

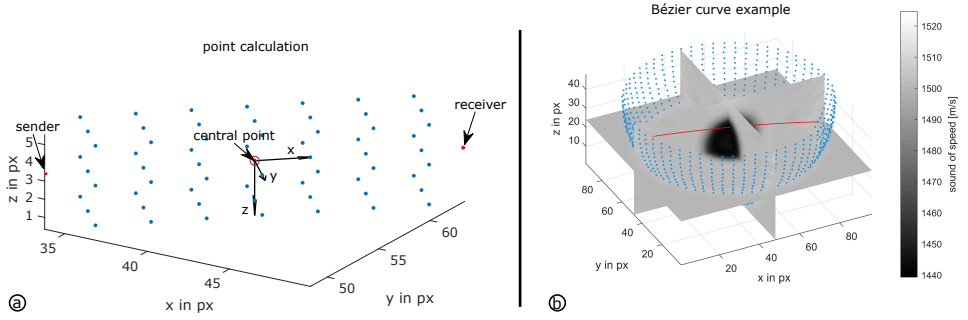


Figure 1: Bézier curve calculation. (a) shows the calculation of the 3D point distribution for determining the set of Bézier curves. It is calculated by the three direction vectors along and orthogonal to the emitter receiver line. The start and endpoint is given by the emitter and receiver ((b), blue points). An example Bézier curve (red) is shown on the underlying first guess sound of speed reconstruction.

$$\begin{aligned}
 \vec{v}_x &= \overrightarrow{P_0P_2} \\
 \vec{v}_y &= \vec{v}_x \times \begin{pmatrix} 0 \\ 0 \\ 1 \end{pmatrix} \\
 \vec{v}_z &= \vec{v}_x \times \vec{v}_y .
 \end{aligned} \tag{2}$$

The selection of the optimal curve is based on a sound speed map. As a first guess, the sound speed map reconstructed with straight rays is used. For each discretized point of the curve the corresponding sound speed value (c_t) is obtained via linear interpolation and the euclidean distance between the sample points is calculated to determine la_t in equation 3. The TOF of an ultrasound pulse travelling along each curve is then defined by:

$$TOF = \sum_{t=1}^{t=k} \left(\frac{1}{c_t} la_t \right) . \tag{3}$$

The curve with the lowest TOF is selected as the optimal one following Fermat's principle [9]. An example curve on an underlying sound speed map is shown in Fig. 1 (b).

2.2 Reconstruction

The image reconstruction is formulated as a linear equation system

$$\vec{b} = M\vec{x} . \tag{4}$$

For reconstructing the sound speed image \vec{x} , the equation system needs to be solved for \vec{x} given the measured time of flight \vec{b} and the system matrix M . It is solved iteratively by an algebraic reconstruction technique using total variation minimization (TVAL3 algorithm [10, 11]). The time of flight values $\vec{b} = (b_1, \dots, b_m)^T$ are gained by calculating the time differences of the recorded signal between the patient measurement and an empty measurement of each emitter-receiver-combination. Matrix M contains the ray paths which describe the wave propagation. For each emitter-receiver combination the voxel discretized Bézier curve is recorded in M . This results in a matrix size of number of measurements (m) \times number of voxels (n).

Considering the refraction, the reconstruction is an iterative procedure. The solution \vec{x} is taken as the new sound speed map on which the Bézier curve method is applied on and M is updated accordingly. By solving the equation system a new estimate for \vec{x} is generated. This proceeding is repeated until convergence (change between iterations $< \epsilon$) or the number of maximum iterations is reached.

3 Results

3.1 2D Evaluations

Before applying the method to 3D, we analyzed the characteristics of the Bézier curve method in 2D experiments due to decreased computing time. The change of the mean squared error (MSE) over the iterations was analyzed. 20 iterations have been carried out. A simple experimental set up was used, with emitter and receiver arranged circular and an circular sound speed inhomogeneity in the centre (see Fig. 2). For the emitter-receiver-ring a radius of 5 cm has been chosen. 200 emitter and 200 receiver were placed. The center frequency was 2.5 MHz with a bandwidth of 1 MHz. The data had been simulated with k-wave [12]. For this setup the MSE decreases the most on the first iterations. For this reason, the following bent ray reconstructions in 3D have been calculated with one iteration as a trade-off between computing time and accuracy. The minimum MSE for the fast marching bent ray reconstruction was reached in the second iteration with 35,00 m/s, for Bézier it was the tenth iteration with 25,64 m/s (straight ray 74,45 m/s).

Furthermore an experiment with third order Bézier curves had been taken for one exemplary ray. The results have been compared to the path calculated using Fermat's principle for a simple setup (see Fig. 3 top) [13]. The ray of the cubic Bézier curve seems to get closer to the calculated one following Fermat's principle. The length deviation is reduced to 1.2 mm in comparison to 1.9 mm. However, the calculation time for the selected parameters increase around factor 100 as the number of free points doubles and all permutations have to be evaluated in the brute force search. Due to the high computational cost and the relatively low gain by cubic Bézier curves on simple object evaluation, we decided to carry out 3D

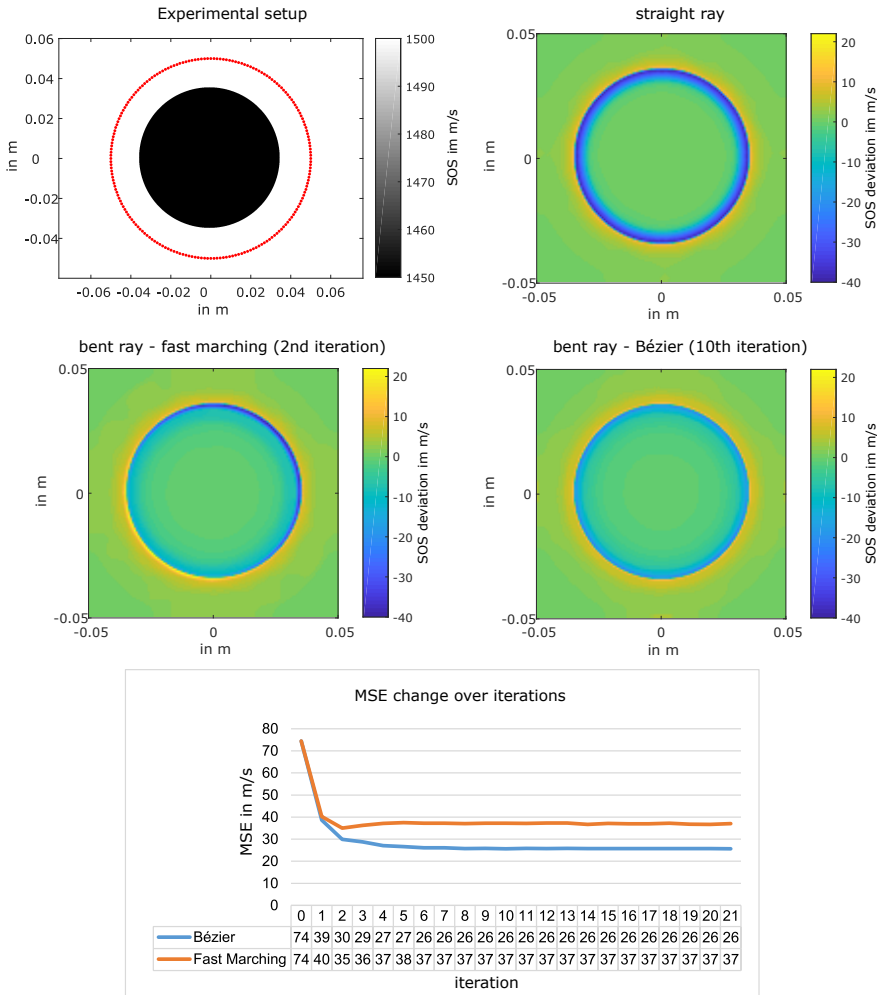


Figure 2: Evaluation of MSE change over iterations. On the upper left the experimental setup is presented, with the emitter/receiver arrangement collar coded red. At the bottom the MSE change over the iterations for Bézier and fast marching is shown. The difference images of zero iteration (straight ray) and the bent ray reconstructions to the reference image are shown.

reconstruction with quadratic Bézier curves. Cubic Bézier curves may be investigated further in future, when a performant GPU implementation is available.

Furthermore the discretization of the Bézier curve, i.e. the step size for t in equation 1 was calculated. The discretization is coupled to the distance in pixels between emitter and receiver. The number of discrete points on the Bézier curve is given by this distance times a factor. Due to the curvature of the Bézier curve, equidistant distribution of t leads to an

irregular point distribution in space, we investigated which factor is required such that the largest distance between two discrete points on the Bézier curve is smaller than half the pixel size in order to fulfill the sampling theorem. With the same experimental 2D setup as before we found that the factor needs to be equal or higher than 3.6.

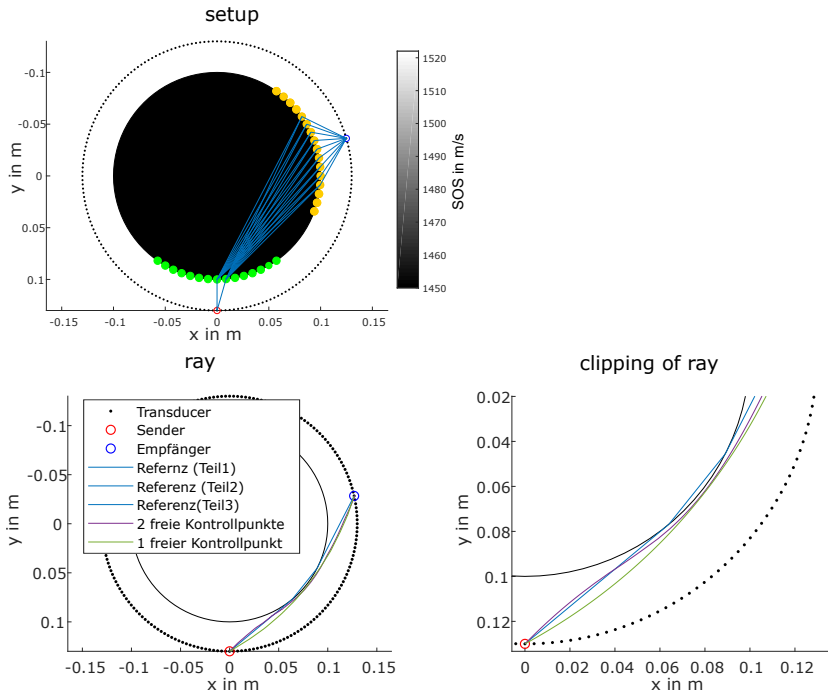


Figure 3: Evaluation of quadratic and cubic Bézier curves. bent rays according to Fermat's principle. Reference beams are calculated using Fermat's principle (top image). The black dots represent the transducers. The example receiver is outlined in blue, the example transmitter is outlined in red. Green or yellow are the discretized points on the circular surface. In blue exemplary paths are given describing possible paths from transmitter to receiver. At the bottom the quadratic and cubic Bézier curves are shown in comparison to the calculated one, with a detailed view on the bottom right.

3.2 Application in 3D

A comparison between Bézier bent ray reconstruction, fast marching bent ray reconstruction and straight ray reconstruction was carried out. For the bent ray reconstruction, one iteration was performed based on the straight ray reconstruction. For the 3D evaluation two datasets are used, one with simulated data and one recorded dataset with KIT 3D USCT [14]. For simulation a simple setup with one sound speed inhomogeneity was selected to examine the main refraction of the water object/tissue interface. In addition more complex phantom data from KIT 3D USCT have been used.

3.2.1 3D k-wave simulation data

For evaluation in 3D simulated A-scan data was used first. We applied a k-wave [12] simulation with a setup of 231 emitter and 1781 receiver. Emitter and receiver are arranged in a hemisphere around a spherical object (0.58 cm diameter) with sound speed inhomogeneity (background: 1500 m/s, object: 1450 m/s). Due to computing time and memory requirements the aperture size with a radius of 1 cm and a depth of 1 cm is smaller than the KIT 3D USCT setup. A center frequency of 2,5 MHz with 1 Mhz bandwidth was chosen. The arrival time of the ultrasound pulse (see equation 3) was calculated via a threshold on the amplitude. The reconstructed image size is $96 \times 96 \times 48$ pixel.

The Bézier curve method produces similar results to the fast marching method. The results are represented for one x/y-, y/z- and x/z-slice in Fig. 4. The mean squared error of the Bézier curve technique is 9.98 m/s in comparison to fast marching (11.85 m/s) and straight ray (15.09 m/s). The standard deviation is 3.63 m/s for straight ray, 3.19 m/s for fast marching and 2.88 m/s for Bézier. The maximum deviation reduces from 48.95 m/s for straight ray to 42.20 m/s for fast marching and 41.09 m/s for Bézier respectively. Both bent ray techniques were able to represent the object size more accurately (see difference image presented in Fig. 4), however differ especially in the speed of sound values in the border regions due to blurring by the total variation regularisation required for the sparse aperture. Especially in the upper z regions the boarder is washed out because of the data sparsity.

3.2.2 KIT 3D USCT phantom data

The methods are also applied on a dataset recorded with KIT 3D USCT [14] with 157 transducer array systems (TAS, containing 4 emitters and 9 receivers each) arranged in a semi-ellipsoidal aperture. The imaged phantom consists of a mixture of gelatine, glycerine and propanol with an approximate sound speed of 1560 - 1570 m/s and an olive placed centrally in the phantom. 10 different aperture positions had been recorded resulting in approximately 500 000 A-scans used for reconstruction. The arrival time was calculated via a cross correlation between measurement with object and empty measurement. The reconstructed image size is $96 \times 96 \times 55$ pixel for a 25.92 cm \times 25.91 cm \times 14.97 cm image.

The straight and bent ray reconstructions are shown in Fig. 5 for three slices. The object size of the phantom in the Bézier bent ray reconstructed image changed similarly to the fast marching reconstructed image. Two region of interests (ROI) have been selected to evaluate the sound speed values of the gelatine mixture. The median of the Bézier curve reconstructed image in the first ROI is 1580.4 m/s in the second one 1564.9 m/s, for fast marching 1574.5 m/s and 1560.4 m/s in comparison to straight ray with 1560.7 m/s and 1560.4 m/s. In the area of the olive higher sound of speed differences can be observed (see Fig. 5).

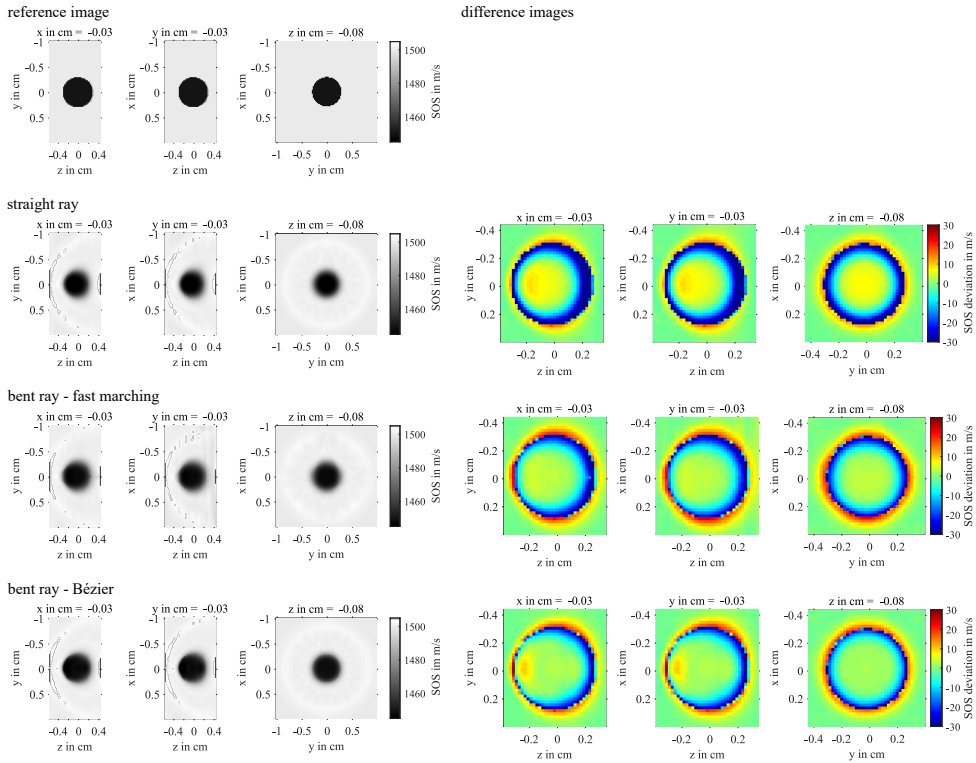


Figure 4: Evaluation of 3D reconstruction with simulated k-wave data. Left column from top to bottom: simulated ground truth, reconstructions with straight ray approximation, fast marching bent ray approximation, and Bézier curve bent ray approximation. The right column shows an enlarged image section of the respective difference to the ground truth with the errors colour coded. Each set of images shows a y/z , x/z and x/y slice from the 3D image.

4 Conclusion

Using Bézier curves for approximating the refraction shows first promising results on 3D simulation data as well as for real data. For simple objects, the Bézier method leads to similar results like the fast marching method. The reconstruction of the object's size improved compared to the straight ray method, the shrinking effect or accordingly the over representation of the object size could be reduced. Bézier curves seem to approximate the main refraction on the object-water interface well. In future, evaluations for more complex objects and real patient data could be carried out to compare the behaviour of the methods. A 3D GPU implementation is currently being developed to compare the computation time for 3D USCT.

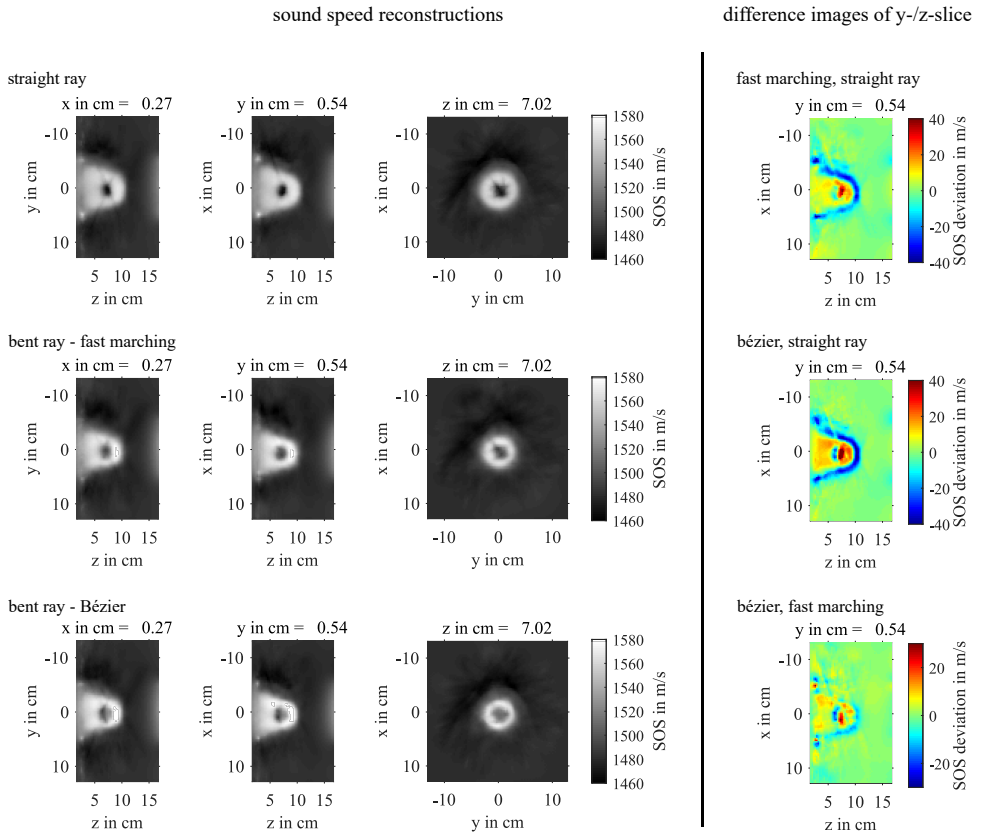


Figure 5: Reconstruction of real experiment data with the KIT 3D USCT. The phantom imaged consists of a mixture of gelatine, glycerine and propanol with an approximate sound speed of 1560 - 1570 m/s. An olive was embedded centrally in the phantom. The images on the left from top to bottom show reconstructed sound speed images with the straight ray approximation, the fast marching bent ray approximation and the Bézier curve bent ray approximation. On the right the sound of speed changes are considered between straight ray and the two bent ray reconstruction.

References

- [1] H. Gemmeke, N. V. Rüter: 3D ultrasound computer tomography for medical imaging. Nuclear Instruments and Methods in Physics Research Section A: Accelerators, Spectrometers, Detectors and Associated Equipment 580(2) (2007), 1057-1065.
- [2] J. F. Greenleaf, R. C. Bahn: Clinical imaging with transmissive ultrasonic computerized tomography. IEEE Transactions on Biomedical Engineering, (2) (1981), 177-185.
- [3] M. Perez-Liva, J. Udias, J. Camacho, J. Herraiz: Real-Time Ultrasound Transmission Tomography based on Bézier Curves. Proceedings of the International Workshop on Medical Ultrasound Tomography (2018), 89-98.

- [4] N. Rüter: Dreidimensionale Ultraschall-Computertomographie: vom Konzept zur klinischen Anwendung. Habilitation Karlsruher Institut für Technologie, (2016).
- [5] J. A. Bærentzen: On the implementation of fast marching methods for 3D lattices (2001).
- [6] M. S. Hassouna, A. A. Farag: MultiStencils Fast Marching Methods: A Highly Accurate Solution to the Eikonal Equation on Cartesian Domains. *IEEE Transactions on Pattern Analysis and Machine Intelligence* 29(9) (2007), 1563–1574.
- [7] M. Perez-Liva.: Time domain image reconstruction methods for transmission ultrasound computed tomography. PhD Thesis University Complutense of Madrid (2017).
- [8] A. R. Forrest: Interactive interpolation and approximation by bézier polynomials. *The Computer Journal*, 15(1) (1972), 71–79.
- [9] M. Born, E. Wolf: Principles of optics: electromagnetic theory of propagation, interference and diffraction of light. Elsevier (2013).
- [10] C. Li: Compressive Sensing for 3D Data Processing Tasks: Applications, Models and Algorithms. PhD thesis, Rice University Houston (2011).
- [11] R. Dapp, M. Zapf, N. V. Rüter: Geometry-independent speed of sound reconstruction for 3D USCT using apriori information. *Proceedings IEEE Ultrasonics Symposium* (2011), 1403–1406.
- [12] B. E. Treeby, J. Jaros, P. Rendell, B. T. Cox: Modeling nonlinear ultrasound propagation in heterogeneous media with power law absorption using a k-space pseudospectral method. *The Journal of the Acoustical Society of America* 131(6) (2012), 4324–4336.
- [13] T. Hopp et al.: Experimental evaluation of straight ray and bent ray phase aberration correction for USCT SAFT imaging. *Medical Imaging 2018: Ultrasonic Imaging and Tomography*, SPIE (2018) 17.
- [14] N. V. Rüter, et al.: First results of a clinical study with 3D ultrasound computer tomography. *IEEE International Ultrasonics Symposium (IUS)* (2013), 651-654.